Planta (2020) 251:92
https://doi.org/10.1007/s00425-020-03387-1

ORIGINAL ARTICLE

Genetic attenuation of alkaloids and nicotine content in tobacco (*Nicotiana tabacum*)

Diego Hidalgo Martinez[1] · Raja S. Payyavula[2] · Chengalrayan Kudithipudi[3] · Yanxin Shen[3] · Dongmei Xu[3] · Ujwala Warek[3] · James A. Strickland[3] · Anastasios Melis[1]

Received: 10 February 2020 / Accepted: 28 March 2020 / Published online: 3 April 2020

Abstract

Main conclusion **The role of six alkaloid biosynthesis genes in the process of nicotine accumulation in tobacco was investigated. Downregulation of ornithine decarboxylase, arginine decarboxylase, and aspartate oxidase resulted in viable plants with a significantly lower nicotine content.**

Abstract Attenuation of nicotine accumulation in *Nicotiana tabacum* was addressed upon the application of RNAi technologies. The approach entailed a downregulation in the expression of six different alkaloid biosynthesis genes encoding upstream enzymes that are thought to function in the pathway of alkaloid and nicotine biosynthesis. Nine different RNAi constructs were designed to lower the expression level of the genes that encode the enzymes arginine decarboxylase, agmatine deiminase, aspartate oxidase, arginase, ornithine decarboxylase, and SAM synthase. *Agrobacterium*-based transformation of tobacco leaves was applied, and upon kanamycin selection, T0 and subsequently T1 generation seeds were produced. Mature T1 plants in the greenhouse were topped to prevent flowering and leaf nos. 3 and 4 below the topping point were tested for transcript levels and product accumulation. Down-regulation in arginine decarboxylase, aspartate oxidase, and ornithine decarboxylase consistently resulted in lower levels of nicotine in the leaves of the corresponding plants. Transformants with the aspartate oxidase RNAi construct showed the lowest nicotine level in the leaves, which varied from below the limit of quantification (20 µg per g dry leaf weight) to 1.3 mg per g dry leaf weight. The amount of putrescine, the main polyamine related to nicotine biosynthesis, showed a qualitative correlation with the nicotine content in the arginine decarboxylase and ornithine decarboxylase RNAi-expressing transformants. A putative early senescence phenotype and lower viability of the older leaves was observed in some of the transformant lines. The results are discussed in terms of the role of the above-mentioned genes in the alkaloid biosynthetic pathway and may serve to guide efforts to attenuate nicotine content in tobacco leaves.

Keywords Alkaloids · Gene expression · *Nicotiana tabacum* · Nicotine · Putrescine · RNAi

Abbreviations

ADC	Arginine decarboxylase
AIC	Agmatine deiminase
AO	Aspartate oxidase
ARG	Arginase
ODC	Ornithine decarboxylase
SAM	S'adenosyl-L:-methionine
WT	Wild type

Electronic supplementary material The online version of this article (https://doi.org/10.1007/s00425-020-03387-1) contains supplementary material, which is available to authorized users.

✉ Anastasios Melis
melis@berkeley.edu

[1] Department of Plant and Microbial Biology, University of California, Berkeley, CA 94720-3102, USA

[2] Eurofins Lancaster Laboratories, Professional Scientific Service Division, 2425 New Holland Pike, Lancaster, PA 17605, USA

[3] Biotechnology Division, Altria Client Services LLC, 601 East Jackson Street, Richmond, VA 23219, USA

Introduction

Plant alkaloids comprise a large group of nitrogen-containing metabolites that are widely distributed throughout the plant kingdom. Alkaloids of *Nicotiana tabacum* L. (tobacco), and especially so that of nicotine, are secondary metabolites that have, since long ago, attracted widespread attention in biology, commerce, society, and medicine (Tso and Jeffrey 1961; Leete 1977; Waller and Nowacki 1978; Baldwin 1989; Dewey and Xie 2013; Patra et al. 2013). Commercial tobacco cultivars typically produce alkaloids at levels between 2 and 6% of the total dry biomass weight. In typical commercial tobacco plants, nicotine accounts for about 90% of the total alkaloid pool (Tayoub et al. 2015; Moghbel et al. 2017), with the secondary alkaloids nornicotine (a demethylated derivative of nicotine), anatabine, and anabasine making up most of the remainder (Saitoh et al. 1985; Sisson and Severson 1990). Recent advances in sequencing and molecular biology have led to the characterization of the majority of the genes coding for the enzymes that are responsible for the biosynthesis of these secondary metabolites (Dewey and Xie 2013).

Availability of the genome sequence of tobacco and the knowledge of many of the structural and regulatory genes involved in the nicotine biosynthetic pathway (Kajikawa et al. 2017) afforded the possibility of manipulating tobacco gene expression to perturb biosynthetic pathways and, thereby, alter the leaf alkaloid content. For example, Kajikawa et al. (2017) reported on phylogenetic and expression analyses, which revealed a series of structural genes of the nicotine biosynthetic pathway, forming a regulon and operating under the control of jasmonate-responsive ETHYLENE RESPONSE FACTOR (ERF) transcription factors.

Putrescine, an important polyamine precursor, is thought to be derived from ornithine via the activity of the enzyme ornithine decarboxylase (ODC) and possibly from arginine via the activity of the arginine decarboxylase (ADC). Putrescine may serve as the reactant to generate the pyrrolidine ring of nicotine in *Nicotiana tabacum* and related species. To test for the arginine biosynthetic route in *N. tabacum*, Chintapakorn and Hamill (2007) used an antisense approach with the hairy root culture system of tobacco, to down-regulate ADC activity in transformant plants. They found concentrations of nicotine to be comparable in antisense-ADC and control lines throughout most of their respective culture cycles, except at the later stages of growth, when the nicotine content of ADC-antisense lines was ~ 20% lower than that of the controls (Chintapakorn and Hamill (2007). They found levels of anatabine, the second most abundant alkaloid typically in *N. tabacum*, to be slightly elevated in two ADC-antisense lines at the latter stages of their culture cycles compared to controls. Their work suggested that the ADC mediated route to putrescine plays a role, but is not of primary importance, in providing the pyrrolidine ring for nicotine synthesis.

To test for the ornithine biosynthetic route in *N. tabacum*, DeBoer et al. (2011) used RNAi methodology with the hairy root culture system to down-regulate ODC transcript levels in *N. tabacum*. They observed a marked effect upon the alkaloid profile of transgenic tissues, with ODC transcript down-regulation leading to lower nicotine (about − 50%) and increased anatabine levels (about + 400%) in both cultured hairy roots and greenhouse-grown leaves. They concluded that the ornithine metabolite and the ODC-catalyzed biosynthetic pathway to putrescine is more important than the ADC-mediated pathway in nicotine biosynthesis and in defining the nicotine:anatabine ratio in *N. tabacum.* These findings were further validated by DeBoer et al. (2013), who showed that RNAi-mediated down-regulation of the ornithine decarboxylase (ODC) expression in *Nicotiana glauca* hindered the well-known wound-stress stimulation of nicotine and anabasine biosyntheses and accumulation.

In the present work, a systematic effort was undertaken to apply RNAi technology and to down-regulate the expression of several alkaloid biosynthesis-related genes in *Nicotiana tabacum*, including the arginine decarboxylase, agmatine deiminase, aspartate oxidase, arginase, ornithine decarboxylase, and S'adenosyl-L:-methionine (SAM) synthase in an attempt to contribute to this body of the scientific literature and to arrive at a more integrated understanding of the interplay between these different genes and pathways in nicotine biosynthesis and accumulation. The results are discussed in terms of a pathway model for alkaloid biosynthesis in tobacco.

Materials and methods

Plant material

The plant material employed in this work was *Nicotiana tabacum*, cv K326-ALCS3 (wild-type tobacco). Seeds were provided by the Altria Client Services, Inc., Richmond, VA, USA. Plantlets in Dixie cups on agar were obtained after seed germination and initial growth on solid (Murashige and Skoog 1962) agar media, supplemented with vitamins and 30 g L^{-1} sucrose. Seedlings were maintained at 24 °C under a 16-/8-h photoperiod (Fig. 1a).

For stable transformation, 1-cm × 1-cm leaf pieces from these tobacco seedlings were infected with transgenic *Agrobacterium tumefaciens* upon immersing the leaves for 5 min in 25 mL YEB cell suspension containing 1 g L^{-1} yeast extract, 5 g L^{-1} meat extract, 5 g L^{-1} bacto peptone, 5 g L^{-1}

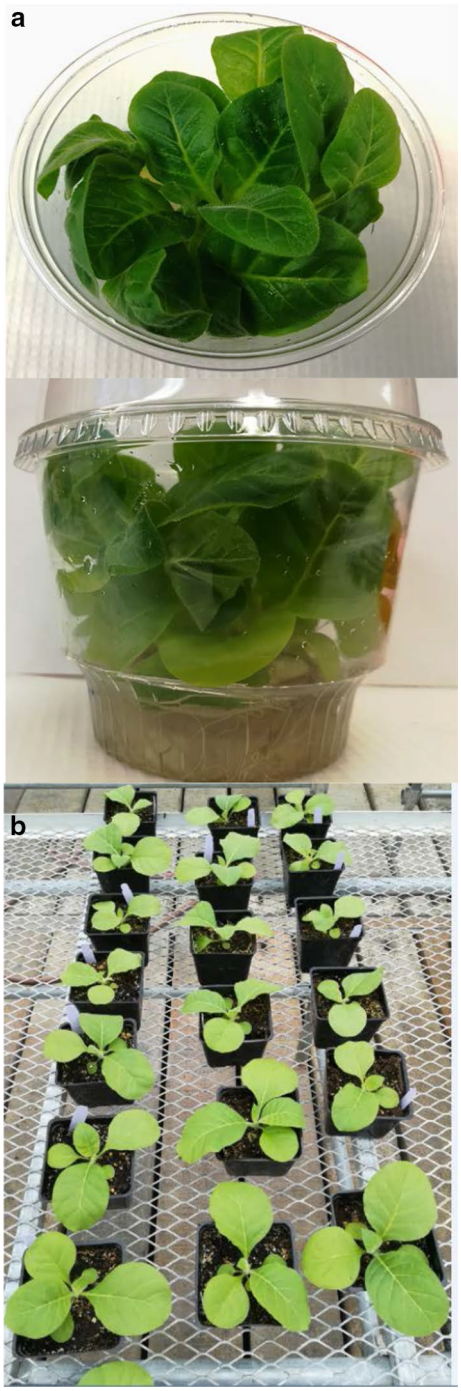

Fig. 1 **a** *Nicotiana tabacum* (tobacco) plantlets in Dixie cups on agar were obtained after seed germination and initial growth on solid Murashige and Skoog agar media, supplemented with vitamins and 30 g L^{-1} sucrose. Seedlings were maintained at 24 °C under a 16-/8-h photoperiod. **b** Rooted transformants, after approximately 5 weeks of growth in Dixie cups, were transferred to soil in the greenhouse and cultivated autotrophically under ambient sunlight conditions

sucrose, 492.8 mg L^{-1} $MgSO_4$-$7H_2O$, plus 0.2 mM of acetosyringone, pH 6.8. The optical density (OD_{600}) of the *A. tumefaciens* cells in the YEB media was between 0.8 and 1. After immersing, the leaf pieces were dried upon gentle blotting with sterile Whatman paper, then transferred to Petri agar plates containing MS media and incubated in the dark for 2 days.

For selection and regeneration, the treated leaf pieces were transferred to agar plates containing MS media supplemented with 500 mg L^{-1} cefotaxime, 150 mg L^{-1} kanamycin, 1 mg L^{-1} 6-benzylaminopurine (BA), 1 mg L^{-1} thiamine-HCl and 100 mg L^{-1} myoinositol. Three rounds of transfer under selection (2-week duration each) were sufficient to enable rooting of the regenerants, upon which the latter were transferred to MS agar media in Dixie cups containing 500 mg L^{-1} cefotaxime and 150 mg L^{-1} kanamycin. The plantlets obtained after these steps of selection and regeneration in the presence of kanamycin were considered to be the T0 transformant lines.

Rooted transformants, after approximately 5 weeks of growth in the Dixie cups, were transferred to soil in the greenhouse and cultivated under ambient sunlight conditions (Fig. 1b). After flowering, T1 seeds were collected, sterilized, cataloged, germinated under kanamycin selection, and individually cultivated in Dixie cups on agar in the presence of 150 mg L^{-1} kanamycin. These T1 plantlets were later transferred to the greenhouse, as the T1 transformant generation. The entire process is pictorially summarized in Fig. S1.

Topping of the T1 tobacco plants in the greenhouse was performed when they started to flower. In this approach, the flower head and the shoot down to the first completely expanded leaf from the top were removed. After 2 weeks of further growth and leaf expansion, the third and fourth leaves from the top were harvested for analysis.

Bacteria and plasmids

To transform the tobacco plants, ten strains of *Agrobacterium tumefaciens* LBA4404 were used: the wild-type control and nine engineered strains carrying the binary plant expression vector p45-2-7-1 with the respective nucleotides encoding the RNAi sequences and the sequence for antibiotic selection (kanamycin) to serve as the selectable marker in both bacteria and plant transformants. These sequences were preceded by the constitutive Cassava Vein Mosaic Virus (CsVMV), serving as the promoter, and followed by the nopaline synthase gene (NOS) terminator.

The RNAi designs were based on the transcript sequences that encode the proteins listed in Table 1. The coding regions of the genes of interest [*Ornithine decarboxylase*, ODC; *Arginine decarboxylase*, ADC; *Aspartate oxidase*, AO; *S-adenosylmethionine synthetase*, SAMS; *Agmatine deiminase*, AIC; *Arginase*, ARG] were retrieved from our in-house NT3.1 database. The cDNA sequences of the above-mentioned genes, and the RNAi construct design

Table 1 Gene name, GenBank ID, and locator number for the alkaloid biosynthesis genes manipulated in this work. RNAi constructs were designed (please see Supplementary materials, page 12) and through *Agrobacterium tumefaciens* transformation were installed in the nuclear genome of *Nicotiana tabacum*

Gene name, GenBank ID, and locator number	Protein name	RNAi designation	*Agrobacterium tumefaciens* construct
ADC-1a: NM_001325190.1 (g67073) ADC-1b: XM_016577301.1 (g1739)	Arginine decarboxylase	ADC	At-ADC
AIC-1a: XM_016610112.1 (g78883) AIC-1b: XM_016615863.1 (g61368)	Agmatine deiminase	AIC	At-AIC
AO-1: XR_001648132.1 (g34809) AO-2a: XM_016595053.1 (g34814) AO-2b: XM_016633697.1 (g83551)	Aspartate oxidase	AO1 AO2	At-AO1 At-AO2
Arginase-1a: XM_016589408.1 (g76552) Arginase-1b: XM_016589407.1 (g29644)	Arginase	ARG	At-ARG
ODC-1a: NM_001325697.1 (g49499) ODC-1b: AF233849.1 (g65779)	Ornithine decarboxylase	ODC	At-ODC
SAMS-1a: XM_016641833.1 (g95117) SAMS-1b: XM_016625263.1 (g23092) SAMS-2a: XM_016583083.1 (g22730) SAMS-2b: AF321140.1 (g94670) SAMS-3a: XM_016608142.1 (g10384) SAMS-3b: NM_001325403.1 (g41661)	SAM synthase	S1 S2 S3	At-S1 At-S2 At-S3

along with the corresponding nucleotide sequences are given in the Supplementary Materials for this work. For each gene of interest, a unique region of about 230–350 bp was selected and inserted in the forward and reverse orientation across the second intron of *Arabidopsis thaliana Actin-11* gene (GenBank accession # BT005593.1), respectively. The entire cassette was synthesized at GenScript (Piscataway, NJ, USA) and cloned under the control of the Cassava vein mosaic virus promoter and *nopaline synthase*-terminator. The binary vector contained the kanamycin resistance gene, *NPTII*, for transgenic plant selection. The plasmid sequences were verified by PCR and Sanger sequencing using two sets of primers: CSVMV-F (CCAGAAGGTAATTATCCAAG) with Intron-R ACAAAGCCAAGAAAGGGTACT, and Intron-F AGATCTTCAACACCTACACCATT with NosT-R AGTTGCTCGAGGAATTCCCG. The plasmids were then transformed into *Agrobacterium tumefaciens* and positive clones were used for the transformation of tobacco. The aspartate oxidase and SAM synthase entailed the design, construction, and use of two and three different RNAi constructs, respectively. A single RNAi construct was employed for the other RNAi constructs.

Agroinfiltration

About 15-cm tall greenhouse-cultivated tobacco plants at about the same developmental stage were used for transient expression experiments with the various RNAi constructs. For infiltration, an overnight culture of *Agrobacterium tumefaciens,* with cells grown at 28 °C, was centrifuged and the cell pellet was resuspended in agroinfiltration buffer (10 mM MES, pH 5.7, 10 mM $MgCl_2$, and 0.2 mM acetosyringone) to a final $OD_{600} = 0.5$. Cells were incubated in this medium for 3 h without shaking. A minimum of three leaves per *Agrobacterium* type, including the wild-type control, were infiltrated by pressing the tip of a 3-mL sterile syringe with the *Agrobacterium* mix into the abaxial side of the leaves (Fig. 2). The agroinfiltrated leaves were harvested 2 days later, frozen in liquid nitrogen and subsequently kept at − 80 °C until use.

Alkaloid extractions

Total leaf alkaloid extractions were made using fresh or frozen leaf material. Fresh leaf pieces of 1 cm × 1 cm or 50 mg of freeze-dried leaf material were macerated in 1 mL of 100% methanol and incubated in the presence of this solvent for 2 h. During this time, the samples were subjected to an ultrasonic ice-water bath. Following a brief centrifugation (10,000 g for 3 min at room temperature) to pellet debris, the supernatant was collected and acidified with 500 µL of 2% (v:v) H_2SO_4, and the hydrophobic neutral compounds were removed with $CHCl_3$ (2 × 500 µL). The remaining polar fraction was subsequently basified upon the addition of 200 µL NH_4OH (25%), and alkaloids extracted with $CHCl_3$ (3 × 500 µL). The organic solvent ($CHCl_3$) was evaporated, and the samples were dissolved in pure methanol prior to gas chromatography (GC), or in phosphate buffer solution (71.6 g L^{-1} of Na_2HPO_3, pH 4.7) for colorimetric analysis.

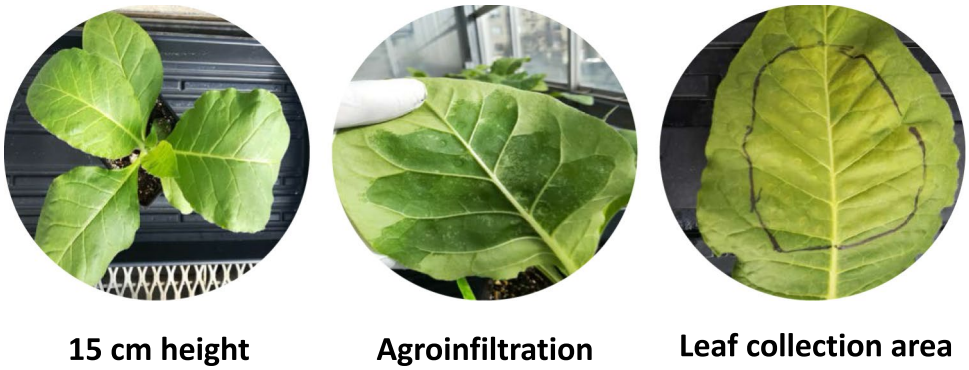

Fig. 2 Transient expression upon in vitro agroinfiltration of *Nicotiana tabacum* (tobacco) leaves with *Agrobacterium* transformants comprising the RNAi constructs used in this work. A minimum of three leaves per *Agrobacterium* transformant, including the wild-type control, were infiltrated by pressing the tip of a 3-mL sterile syringe with the *Agrobacterium* mix into the abaxial side of the leaves. Samples were collected for analysis 48 h after the agroinfiltration

Total alkaloid quantifications

A spectrophotometric method, developed by Patel et al. (2015), was applied with some modifications. Briefly, alkaloids extracted from each single fresh leaf disc (1.5 cm diameter) were resuspended in 200 µL phosphate buffer solution (pH 4.7), mixed with 200 µL bromocresol green solution (BCG) (1 mM stock), then 400 µL of chloroform was added to extract the alkaloids. Finally, the absorbance spectrum of the solution was measured in the 350–550 nm region with a UV–VIS Shimadzu UV-1800 spectrophotometer (Fig. 3, upper). A calibration curve was constructed of the absorbance maximum at 415 nm, as a function of the concentration of nicotine in the solution. Nicotine was selected as the molecule of choice for this calibration curve, as it is the most abundant alkaloid in tobacco leaves. The calibration curve served as a standard, comprising 0.375, 0.75, 1.50, 3, 6 and 12 µg nicotine in 400 µL volume (Fig. 3, lower). As nicotine comprises > 90% of all leaf alkaloids, this calibration curve was applied in total alkaloid quantification (nicotine equivalents).

Direct nicotine detection and quantification

To quantify the specific level of nicotine in the leaves, alkaloids extracted from 50 mg of freeze-dried material were subjected to a GC-FID analysis with a Shimadzu GC-2014 Gas Chromatography apparatus equipped with a flame-ionization detector (FID). A fused silica capillary column of 30 m, 0.32 mm ID and 0.25 µm of film thickness (Rtx-5 Resteck) was used with N_2 as the carrier gas at a flow rate of 1 mL min^{-1}. The temperature profile was 60 °C, followed by a temperature rate increase of 12 °C min^{-1} up to 290 °C. The injector and detector temperatures were set to 290 °C, the injection volume was 8 µL and the split was set at 20:1

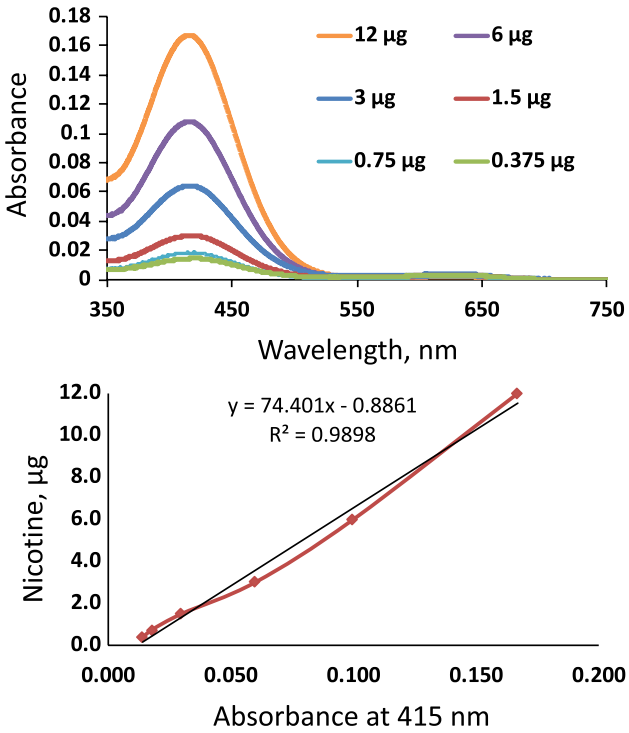

Fig. 3 Spectrophotometric determination of total alkaloid leaf extracts from *Nicotiana tabacum* (tobacco). Upper panel: absorbance spectrum of the alkaloid-containing solution measured in the 350–550 nm region defining a 415-nm absorbance band. Lower panel: calibration curve of the absorbance maximum at 415 nm, as a function of the concentration of nicotine in the 400 µL assay solution

(Fig. 4). This analysis showed a linear response of the apparatus to nicotine concentration and a quantification limit of 20 µg nicotine per g dry leaf weight.

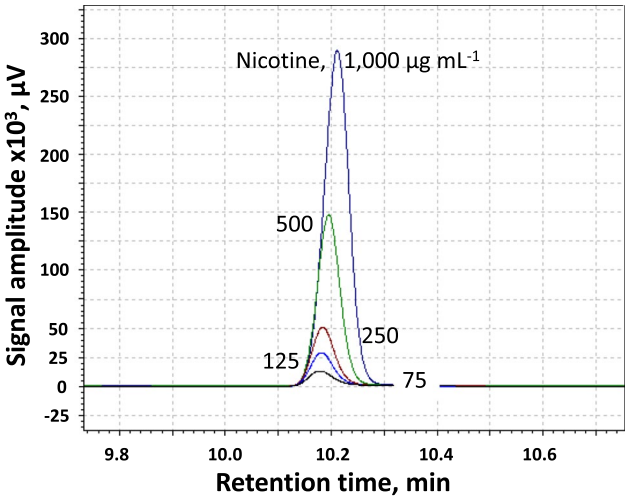

Fig. 4 GC-FID analysis with a Shimadzu GC-2014 Gas Chromatography apparatus equipped with a flame-ionization detector (FID) showing the signal amplitude of the samples with different concentrations of nicotine. The latter had a retention time of 10.2 min under the experimental conditions employed. The analysis showed a linear response of the apparatus to nicotine concentration and a detection limit of 12.5 µg nicotine mL^{-1}

Table 2 Primers specific for the various genes of interest employed in this work

Primer id	Sequence
ODC_qPCR_FW	ACGTTTCCGACGACTGTGTT
ODC_qPCR_RV	GCAGCTCCGGTAACTGGTAA
ADC_qPCR_FW	GTGTCACAGAGCGATAGCCC
ADC_qPCR_RV	TGCTTGAGCGTCTCGAACAT
AO_qPCR_FW	TGTTGTGCCAACCTGGTAGT
AO_qPCR_RV	GTTGGCAACCTCTCGCTTTC
SAM_qPCR_FW	TGACTTCAGGCCTGGAATGAT
SAM_qPCR_RV	CCTTGACAGTCTCCCAGGTG
AIC_qPCR_FW	GGTACAAGGCTTGCTGCTTC
AIC_qPCR_RV	TCTGGAAACGCCAGTGAGAG
Arg_qPCR_FW	GCGGTCTCTCTTTCCGTGAT
Arg_qPCR_RV	GCAGTCATGCCATCAACAGT
ElongationF_FW	TGGTCAGGAGATTGCGAAAGAGC
ElongationF_RV	ACGCAAAACGCTCCAATGGTG
KanR_FW	CAAGATGGATTGCACGCAGG
KanR_RV	TGATATTCGGCAAGCAGGCA

KanR kanamycin resistance

Genomic DNA PCR and RT-qPCR

To identify and verify positive RNAi transformants, the presence of the kanamycin selectable marker was tested by genomic DNA PCR using the Phire Plant Direct PCR Master Mix (Thermo SCIENTIFIC) (Fig. S2). Experimental conditions for the PCR were 95 °C for 5 min, then 35 cycles comprising 95 °C for 60 s; 60 °C for 30 s; 72 °C for 60 s, and 72 °C for 5 min.

Transient expression of the target genes in tobacco leaves after agroinfiltration was verified by resolving the cDNA (RT-qPCR) products in an agarose gel (1%), as detailed in recent work from this lab (Kirst et al. 2018). The elongation factor 1a (EF-1a) was used for expression normalization, as a nuclear-encoded reference gene. For RT-qPCR, 2 µL of cDNA was used and each sample was run in triplicate, under the following conditions: 95 °C for 2 min, then 35 cycles comprising 95 °C for 10 s; 60 °C for 20 s; 72 °C for 20 s, and 72 °C for 2 min.

Total RNA from the plant material was isolated using the TRI Reagent® (Sigma-Aldrich). cDNA was prepared from 1 µg total RNA treated with DNase I, RNase-free (Thermo Scientific) and synthesized with M-MuLV Reverse Transcriptase (New England BioLabs®Inc.). Expression levels in the seedlings were tested with the CFX96 Touch Real-Time PCR Detection System (Bio-Rad). The reaction mix was prepared with Luna® Universal qPCR Master Mix (NEB) and each sample was run in triplicate, under the following conditions: 95 °C for 2 min, then 40 cycles comprising 95 °C for 10 s; 60 °C for 20 s; 72 °C for 20 s, followed by a melting curve. For these experiments, primers specific for the various genes of interest were designed with the assistance of Primer-BLAST (Table 2).

Polyamines extraction and quantification

To extract free polyamines, 250 mg of fresh leaves were homogenized and incubated with 1 mL 5% perchloric acid on ice for 30 min. The mix was centrifuged at 12,000 g for 10 min at 4 °C, and 0.8 mL of the supernatant was transferred to a new 2-mL tube. This supernatant was mixed with 0.8 mL of oversaturated sodium carbonate solution, 40 µL of 0.5 mM 1,7-heptanediamine (HDT), and 10 µL of isobutylchloroformate. Following incubation for 30 min at 35 °C, 200 µL of toluene were added, mixed well, and centrifuged at 10,000*g* for 1 min. Aliquots of 100 µL of the organic layer were used for analysis by GC-FID.

The GC-FID analysis was performed with a Shimadzu GC-2014 Gas chromatography apparatus equipped with a flame-ionization detector (FID), as above. The temperature profile, in this case, was 110 °C, followed by a temperature rate increase of 30 °C min^{-1} up to 320 °C held for 13 min. The injector and detector temperatures were set to 250 °C, the injection volume was 8 µL and the split was set at 15:1. Calibration curves were conducted using putrescine (PUT), cadaverine (CAD), HDT-like internal standard, spermidine (Spd), and spermine (Spm) (Fig. S3). Calibration curves were measured with the above standards at concentrations of

10, 5, 2.5, 1.25 and 0.625 mM for each of these compounds (limit of detection was 0.5 mM).

Statistical analysis

Statistical analysis of the results was performed using the software package Past3.20 (Øyvind Hammer, April 2018). All experimental results were expressed as mean ± standard deviation (SD). Analysis of variance (ANOVA) and mean comparison were performed using Tukey's multiple-range test. A P value of <0.05 was considered to be statistically significant.

Results

Evaluation of transient expression

To obtain an initial evaluation of the effectiveness of the RNAi constructs to downregulate the respective gene expression, leaves from tobacco plants in the same developmental stage were agroinfiltrated for transient expression measurements. Nine different *Agrobacterium tumefaciens* strains (At-ADC, At-AIC, At-AO1, At-AO2, At-ARG, At-ODC, At-SAMS 1, At-SAMS 2, and At-SAMS3) containing the respective RNAi constructs (Table 1) and the control strain were used to inoculate the tobacco plants (see "Materials and methods"). The agroinfiltrated leaves were harvested 2 days later, frozen in liquid nitrogen, and stored at − 80 °C until ready to use. Total RNA was extracted from each leaf sample and RT-qPCR analysis was performed. Levels of gene expression at the mRNA level are reported as the percentage for each gene transcript in the presence of the RNAi construct, compared to those of the control. The following levels were noted (± standard error of the mean): ADC = 88% (± 10%), AIC = 33% (± 28%), AO1 = 63% (± 14%), AO2 = 67% (± 30%), ARG = 84% (± 15%), ODC = 62% (± 15%), SAMS1 = 62% (± 10%), SAMS2 = 70% (± 16%), SAMS3 = 67% (± 17%). These results (Fig. S4) provided an initial assessment of the effect of the RNAi constructs on the corresponding gene expression.

Screening of the genomic transformants

About 120 T0 RNAi and control plants were cultivated, first in Dixie cups on agar in the lab, until they reached a height of about 10 cm. These were selected for antibiotic resistance and further tested by PCR analysis for the presence of the RNAi transgenes (Fig. S2). They were transferred to the greenhouse for growth in soil, and for T1 seed generation by self-fertilization. T1 seeds were harvested, sterilized, and germinated first in Dixie cups on agar in the lab in the presence of kanamycin. Leaf samples from the emanating

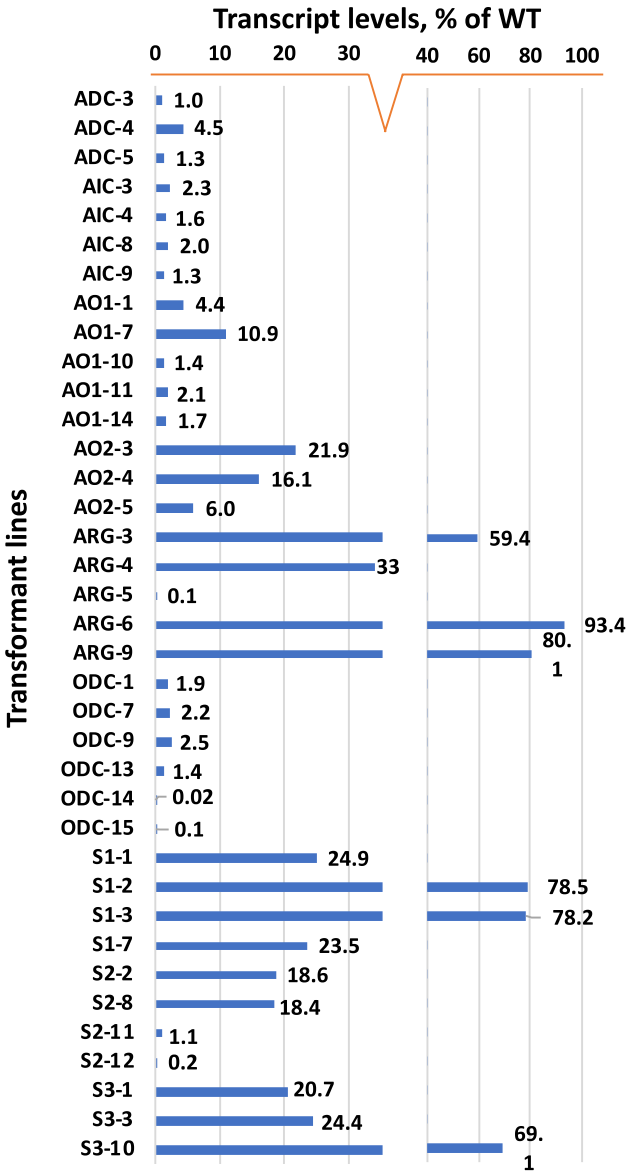

Fig. 5 Transcript levels as a measure of gene expression in T1 RNAi transformant tobacco leaves. The results showed a substantially lower transcript level for all independent event lines derived from the ADC, AIC, AO, and ODC RNAi transformations. The ARG and SAMS transformant lines showed mixed and/or inconsistent results, with some lines having transcript levels comparable to the wild type, while others showed lower levels. Levels of gene expression at the mRNA level are reported as percentage of each gene transcript in the presence of the RNAi construct, compared to those of the control. Each sample was run in triplicate

T1 seedlings were tested to evaluate the level of target gene expression by RT-qPCR (Fig. 5). Transcript levels were plotted as a fraction (%) of the corresponding one in the wild type, thus providing a measure of gene expression in T1 RNAi transformant tobacco plants, and also a measure of the efficacy of the RNAi approach to gene expression downregulation. The results showed a substantially lower transcript

Table 3 RNAi constructs and RNAi transformant lines with the lowest level of transcripts (RT-qPCR analysis) detected in T1 tobacco seedlings (please see "Results" on screening of the genomic transformants)

RNAi construct	Lines with lowest gene expression and low content of total alkaloids
ADC	3, 4, 5
AIC	3, 4, 8, 9
AO1	1, 7, 10, 11, 14
AO2	3, 4, 5
ARG	3, 4, 5, 6, 9
ODC	1, 7, 9, 13, 14,15
SAMS 1	1, 2, 3, 7
SAMS 2	2, 8, 11, 12
SAMS3	1, 3, 10

level, reaching as low as 1% of those in the wild type, for all independent event lines derived from the ADC, AIC, AO, and ODC RNAi transformations (Fig. 5). The ARG and SAMS transformant lines showed mixed and/or inconsistent results, with some lines having transcript levels comparable to the wild type, while others showed substantially lower levels. A minimum of three plants from each transformation event with lower levels of expression of the target genes was selected for further growth in the greenhouse and subsequent analysis. In total, 37 lines comprising the nine RNAi constructs plus the wild type were evaluated. The specific number of transformants by each RNAi construct is shown in Table 3 and Fig. 5 (RNAi transformant lines). Only three lines from independent events were examined for the ADC and AO2, whereas four lines of SAMS1 and six lines from independent events were examined for the ODC RNAi transformants. Intermediate number of lines from independent events were examined in the case of the other RNAi transformants (Table 3).

A preliminary measurement of total alkaloid content was performed in each of the T1 Dixie cup seedlings referenced in Table 3. Figure 6 shows the values for these 37 lines selected to be transferred to the greenhouse. In this early vegetative stage, only the AO1 RNAi lines showed a systematically and substantially lower-than-wild-type alkaloid content. Some of the ODC RNAi lines also showed a statistically significant lowering in total alkaloid content compared to the wild-type control (WT). In contrast, all AO2 and most of the SAMS RNAi lines showed significantly greater alkaloid content values than the WT. A subsequent alkaloid quantification was undertaken later, following the early budding stage, with mature plants grown in the greenhouse (Fig. 7). At this mature plant development stage, the content of total alkaloids in most of the transgenic lines was lower compared to the control (WT), except for some of the AO2

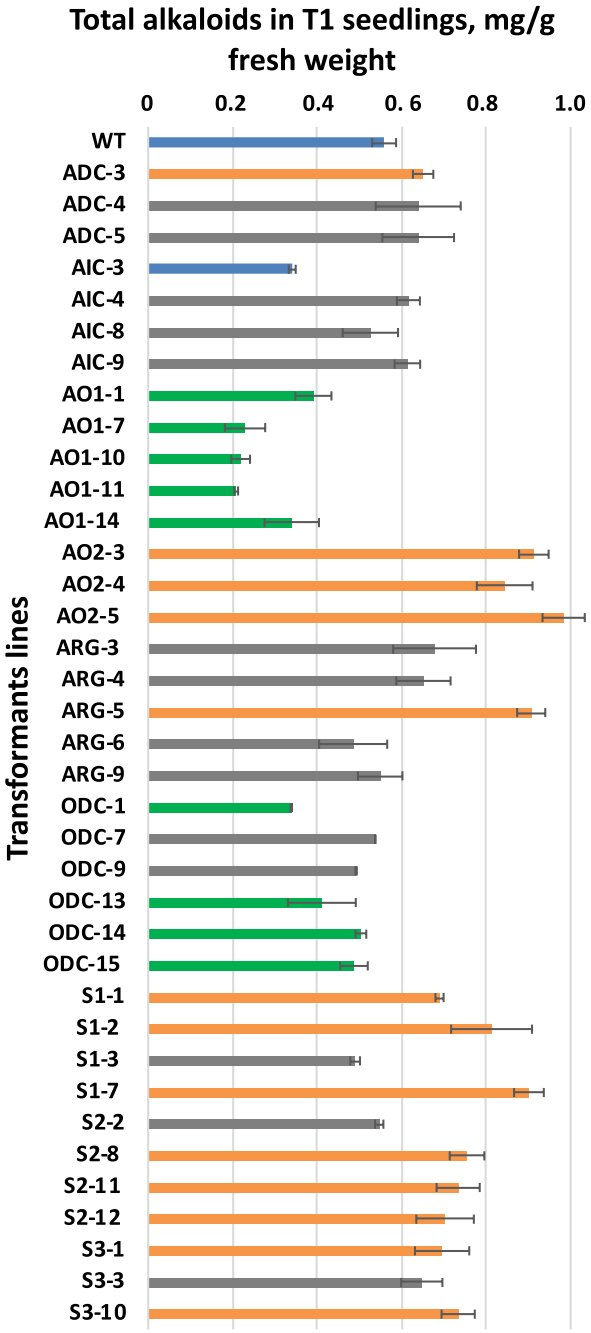

Fig. 6 Total alkaloid content of leaves from 37 independent transformant lines with six different RNAi constructs of T1 plants plus the wild-type control in the early growth phase, while seedlings were still in Dixie cups in the lab. Note that at this early vegetative stage only the AO1 RNAi and some of the ODC RNAi lines showed significantly lower total alkaloids content than the wild type (WT). In contrast, all AO2 and SAMS RNAi lines showed significantly greater alkaloid content values than the WT. Guide to the color-coded bars: Blue bars: alkaloid content of the WT. Orange bars: statistically significant alkaloid content above that of the WT. Grey bars: no statistically significant alkaloid content difference, compared to that of the WT. Green bars: statistically significant alkaloid content below that of the WT. Results are the mean ± SD; $n = 3$

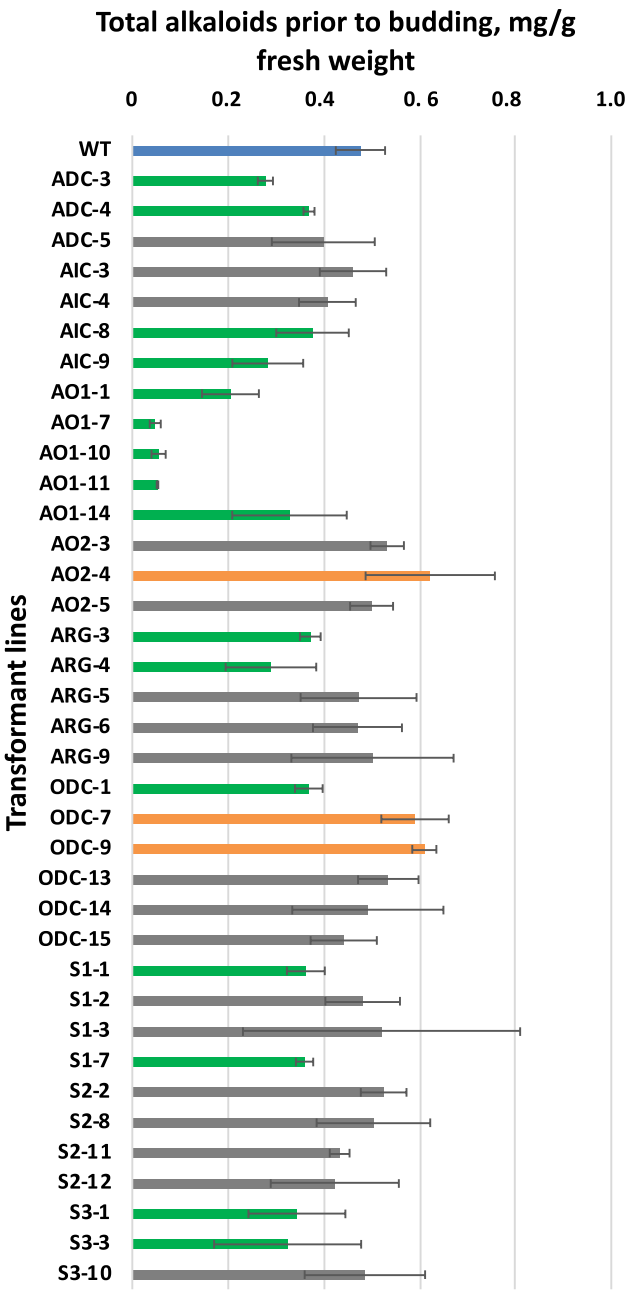

Fig. 7 Total alkaloid content of mature leaves harvested at the greenhouse from 37 independent transformant lines with six different RNAi constructs of T1 plants plus the wild-type control following the early budding plant development stage. The total alkaloid content of all AO1 lines was substantially lower than that of the wild type (WT), whereas other transgenic lines yielded mixed results. Some of the AO2 and ADC lines continued to show significantly greater than wild type values. Guide to the color-coded bars: Blue bar: alkaloid content of the WT. Orange bars: statistically significant alkaloid content above that of the WT. Grey bars: no statistically significant alkaloid content difference compared to that of the WT. Green bars: statistically significant alkaloid content below that of the WT. Results are the mean ± SD; $n = 3$

and ODC lines, which gave mixed results, with some of these lines showing significantly greater than wild-type alkaloid content.

Leaf nicotine analysis

For the quantification of nicotine, the flower head and the shoot down to the first completely expanded leaf from the top were removed. Two weeks after this topping off, the third and fourth leaves from the top were harvested, midrib removed, and the leaves were frozen in liquid nitrogen and lyophilized. The samples were ground and used for total alkaloid extraction. The average nicotine content of the leaves in three biological replicates from each T1 line is shown in Fig. 8. All transformants expressing the AO1-RNAi and AO2-RNAi had the lowest values of nicotine compared to the control (WT). The latter had 3.9 ± 1.3 mg NCT per g DW. The nicotine content range of the AO1-RNAi lines varied from below the limit of quantification (20 µg per g dry leaf weight) to 0.54 ± 0.13 mg per g dry leaf weight. The nicotine content range of the AO2-RNAi lines varied between 0.63 ± 0.3 and 1.3 ± 0.58 mg NCT per g DW. The next most significant suppression of nicotine content was observed in the ODC-RNAi lines 1, 13, 14 and 15. Also, ADC-RNAi had at least two lines with lower than wild-type nicotine content. In contrast, lines AIC-RNAi, ARG-RNAi and SAMS2-RNAi did not display significant differences compared with the wild-type control.

It is of interest that the effect of the AO1 RNAi construct increased with the plant developmental status, going from an average of 0.34 g alkaloids per g FW in the seedling stage (Fig. 6) to as low as 0.06 g alkaloids per g FW in developed leaves harvested just prior to budding (Fig. 7). This was further attenuated later in the development that was measured after plant topping, as evidenced from the near absence of nicotine in these AO1 transformants (Fig. 8).

Polyamine profile

Leaf samples for polyamine determination were taken from the topped-off plants, as was the case of the samples for nicotine analysis. Figure 9a shows the mean putrescine content in the various RNAi lines. Compared to wild type, ADC-RNAi and ODC-RNAi lines had significantly lower content of putrescine, while AIC-RNAi, ARG-RNAi, and SAMS-RNAi lines had levels of putrescine equivalent to that measured in the control (Fig. 9a, WT). AO lines were not tested in this respect because AO functions in a different pathway (please see discussion, below). Putrescine levels seemed to be lower in the ADC-RNAi than the ODC-RNAi lines; however, the difference was not statistically significant and the uncertainty (error bars) in the two measurements prevented drawing an unequivocal conclusion. The

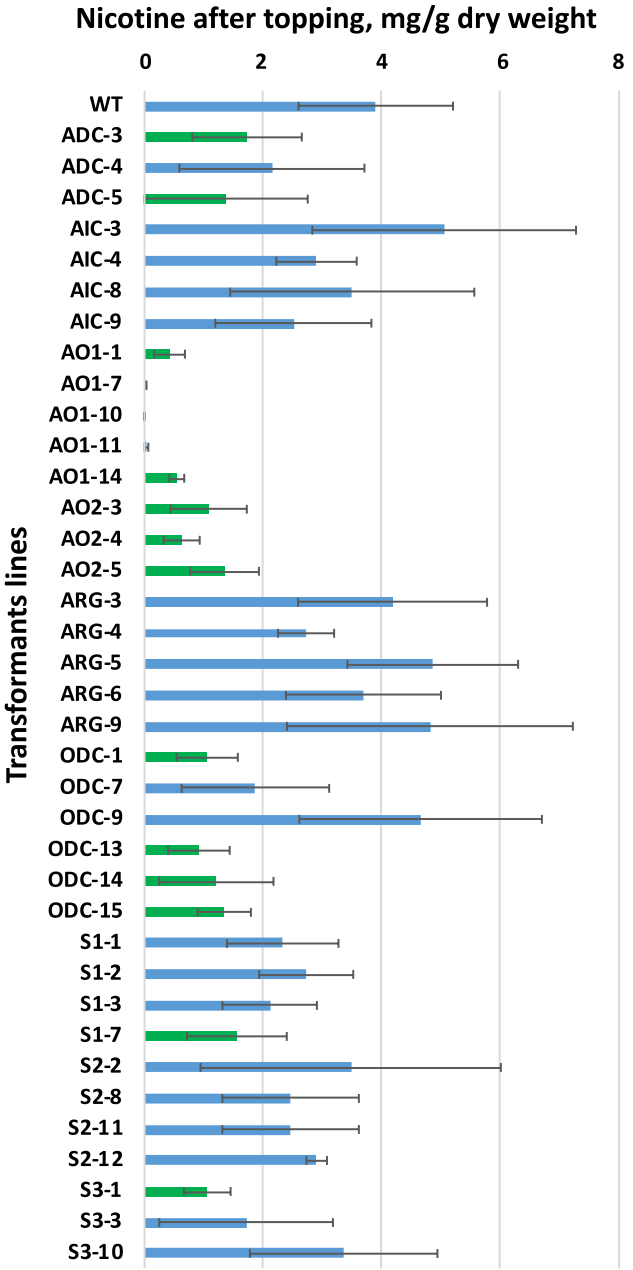

Fig. 8 Nicotine content of leaves from T1 plants grown at the greenhouse. The assay included 37 independent transformant lines with six different RNAi constructs of T1 plants plus the wild-type control 2 weeks after topping. Transformants expressing the AO1-RNAi and AO2-RNAi had the lowest nicotine content compared to the control (WT). The next most significant suppression of nicotine content was observed in the ODC-RNAi lines 1, 13, 14, and 15. Also, ADC-RNAi had at least two lines with lower than wild-type nicotine content. In contrast, lines AIC-RNAi, ARG-RNAi, and SAMS2-RNAi did not display significant differences compared with the wild-type control. Guide to the color-coded bars: Blue bars: no statistically significant nicotine content difference compared to that of the WT. Green bars: statistically significant nicotine content below that of the WT. Results are the mean ± SD; $n = 3$

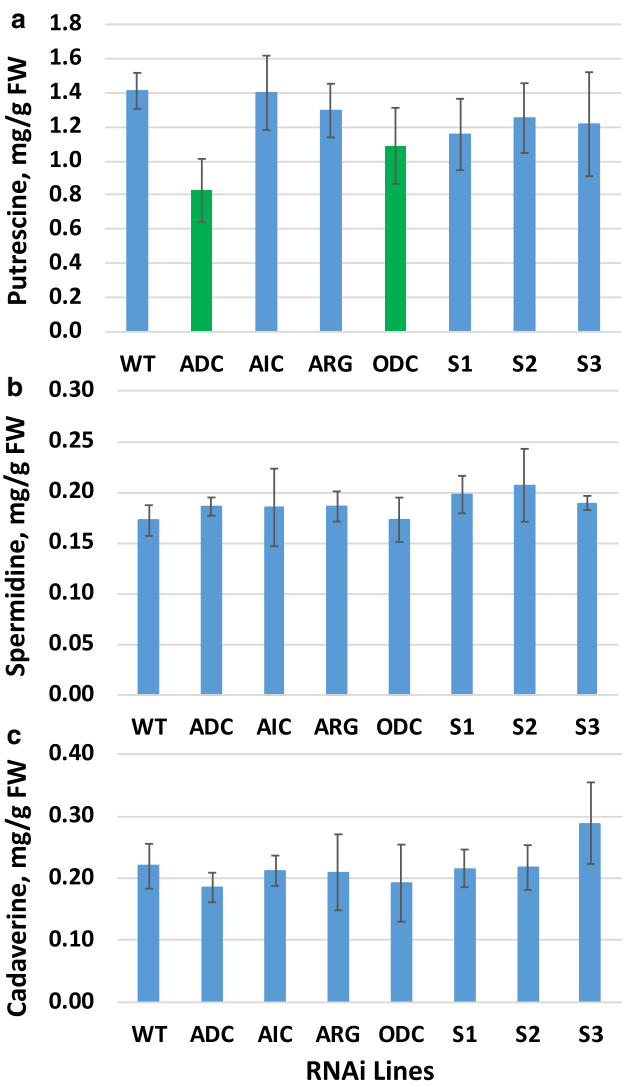

Fig. 9 Mean content of **a** putrescine, **b** spermidine, and **c** cadaverine in each type of RNAi line examined in this work. A minimum of three biological replicates and maximum of six (mean ± SD; $n = 3$–6) were applied to each of the polyamines quantified. The values shown are the average of all the lines for each type of RNAi construct employed. Compared to wild type, ADC-RNAi and ODC-RNAi lines had significantly lower content of putrescine, while AIC-RNAi, ARG-RNAi, and SAMS-RNAi lines had levels of putrescine equivalent to that measured in the control (WT). The spermidine and cadaverine contents of the RNAi transformants were statistically invariable from that of the control. Guide to the color-coded bars: Blue bars: no statistically significant putrescine, spermidine, or cadaverine content difference compared to that of the WT. Green bars: statistically significant putrescine content below that of the WT

spermidine (Fig. 9b) and cadaverine (Fig. 9c) contents of the RNAi transformants were not statistically different from that of the control.

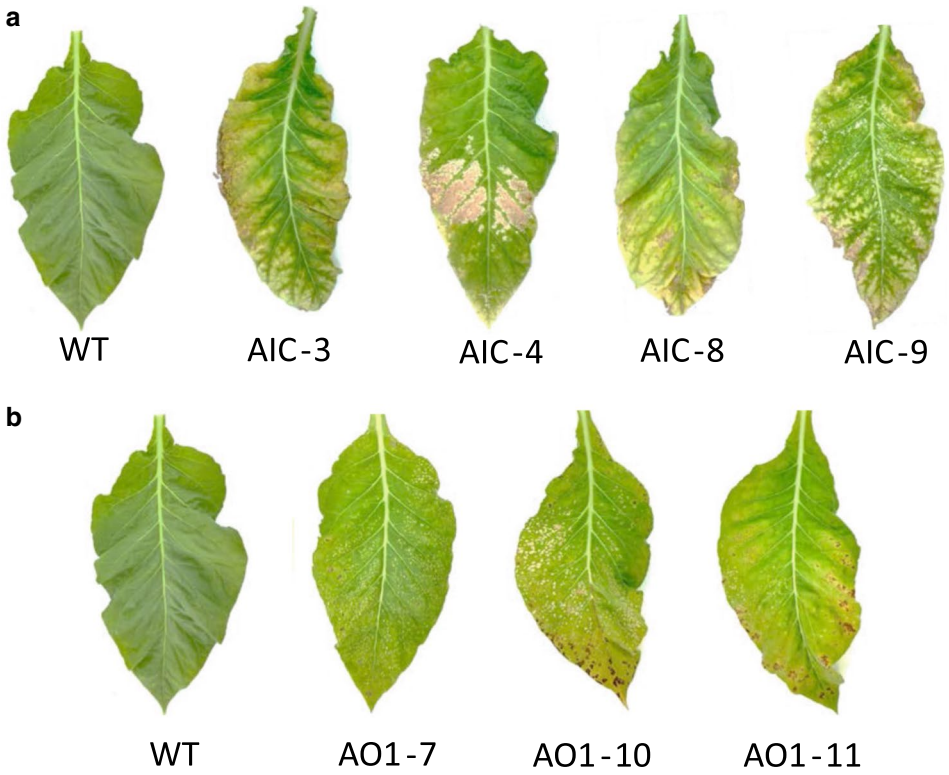

Fig. 10 Phenotypic variation noted for the older leaves in **a** the AIC-RNAi and **b** AO1-RNAi lines. In all AIC-RNAi lines in **a**, the fully expanded and oldest leaves showed signs of early senescence-like discoloration. Similarly, in some of the AO1-RNAi lines in **b**, the fully expanded and older (lower) leaves also showed symptoms of early senescence-like discoloration. Lines that showed this phenotype (AO1 lines 7, 10, and 11) were the ones with the lowest level of nicotine content. It should be noted that these "early" coloration changes affected the oldest leaves of the transformants, as compared with the wild-type control, whereas upper leaves of these plants, including the third and fourth leaves from the top that were harvested for alkaloids and nicotine analyses had a normally green pigmentation and otherwise healthy phenotype, very much like the wild type

Leaf phenotype of the RNAi transformants

Differences in the phenotype of the leaves were noted between the various transformants and the wild-type control. In all AIC-RNAi lines (Fig. 10a), the fully expanded and oldest (lower) leaves showed a premature turning to yellow then reddish-brown coloration. They initially developed concentric ring spots, which expanded and merged to form larger leaf areas of tissue reminiscent of senescence. In general, the photosynthetic viability of the mature and oldest (lower) leaves was negatively affected in the plants expressing the AIC-RNAi construct. This phenomenology was limited to the lower leaves and did not seem to affect the upper leaves of these plants, including those that were sampled for alkaloids, nicotine, and polyamines analysis.

In only some of the AO1-RNAi lines (Fig. 10b), the fully expanded and oldest (lower) leaves also turned yellow, developed white spots, which later became reddish-brown. The lines that developed this phenotype (AO1 lines 7, 10, and 11) were the ones with the lowest level of nicotine content in the upper leaves. Interestingly, none of the AO-2-RNAi plants developed the early senescence phenotype (not shown).

It should be noted that these coloration changes described above affected the oldest leaves of these transformants, whereas higher up leaves, including the third and fourth leaves from the top that were harvested for alkaloids and nicotine analyses, had a normally green pigmentation and otherwise healthy phenotype, very much like the wild-type control.

Discussion

A systematic effort was undertaken to assess the role of a number of alkaloid biosynthesis enzymes in the process of nicotine synthesis and accumulation in *Nicotiana tabacum*. RNAi technology was applied to down-regulate the expression of several alkaloid biosynthesis-related genes in tobacco, including the aspartate oxidase (AO), ornithine decarboxylase (ODC), arginine decarboxylase (ADC), agmatine deiminase (AIC), arginase (ARG), and

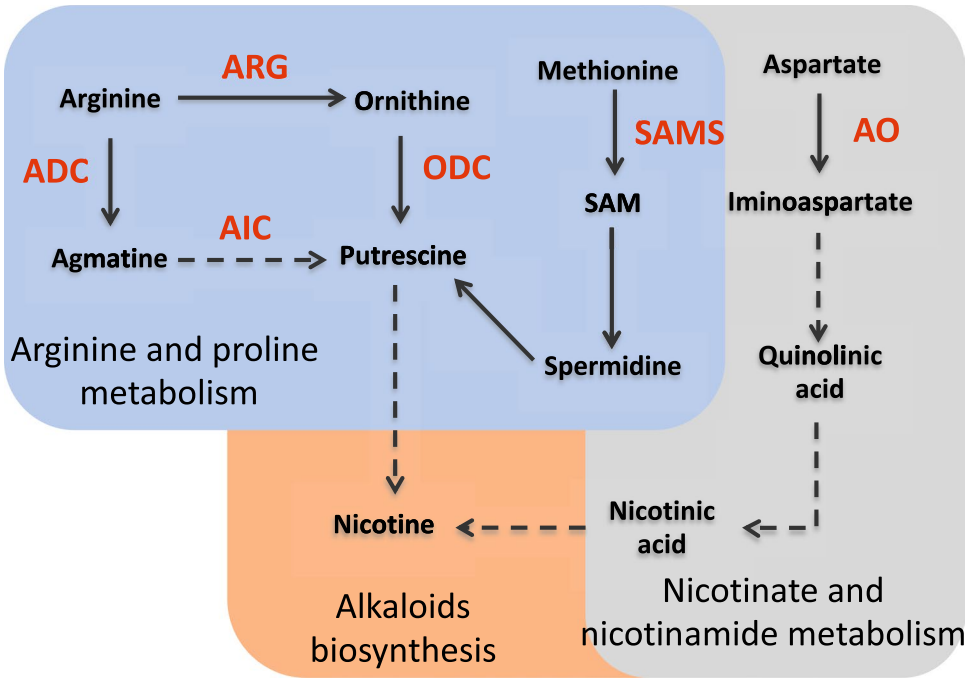

Fig. 11 Putative alkaloid biosynthetic pathway schematic in *Nicotiana tabacum*. Shown are the putative arginine and proline metabolism, alkaloids biosynthesis, and nicotinate and nicotinamide metabolism pathways, as they may be involved in the analysis reported in this work. Schematics are based on pathway information summarized in https://www.genome.jp/dbget-bin/www_bget?R09077+RC00053, https://www.genome.jp/kegg-bin/show_pathway?rn00330, https://www.genome.jp/kegg-bin/show_pathway?rn00960, https://www.genome.jp/kegg-bin/show_pathway?rn00760

S'adenosyl-L:-methionine (SAM) synthase. Results presented in this work showed that nicotine content in tobacco leaves was attenuated the most in plants expressing ADC, ODC, and AO in an RNAi configuration. The ODC results are consistent with the findings of DeBoer et al. (2011, 2013) showing that an ornithine to putrescine reaction (Fig. 11), catalyzed by ODC, is an important step in alkaloid and nicotine biosynthesis and accumulation. The results also showed that the nicotinate and nicotinamide metabolic pathway is also important in the synthesis and accumulation of nicotine, in a putative process schematically shown in Fig. 11. Conversely, the results strengthen the notion that steps of the arginine and proline metabolism and the associated enzymes, including AIC and ARG (Fig. 11), do not play a significant role in determining leaf nicotine levels. An intermediate nicotine attenuation effect was noted upon the RNAi-mediated down-regulation of SAM synthase enzymes, suggesting that methionine to spermidine to putrescine may also contribute to nicotine synthesis and accumulation. In sum, results from this work suggested that multiple different biosynthetic pathways catalyzed by a variety of different enzymes may feed substrate toward nicotine biosynthesis in commercial cultivars of tobacco.

The complexity of the alkaloids and nicotine biosynthetic pathways shown in Fig. 11 could be seen in light of the origin of the tobacco species employed in this work. *Nicotiana tabacum* is a tetraploid species that originated from the natural hybridization of two *Nicotiana* diploid species, i.e., *N. tomentosiformis* and *N. sylvestris* (Goodspeed and Clausen 1928; Smith 1968; Gray et al. 1974; Kung et al. 1975). Gray et al. (1974) and Kung et al. (1975) employed an analysis of the polypeptide composition of fraction I protein in *Nicotiana tabacum* to show the distinct origin of subunits from two species, thereby supporting the hypothesis of a natural hybridization of two *Nicotiana* species (*N. tomentosiformis* and *N. sylvestris*) to yield what is now the commercial cultivars of *Nicotiana tabacum*. Similarly, Bai et al. (2011) reported on two flavonoid-related basic helix-loop-helix regulators, NtAn1a and NtAn1b, of tobacco as originating from two *Nicotiana* ancestors that are functional but independently active. It is tempting to speculate that distinct nicotine biosynthetic pathways originated in the two different diploid tobacco species, i.e., *N. tomentosiformis* and *N. sylvestris*, and they now coexist but differentially regulated, e.g. by environmental and developmental conditions (Payyavula et al. 2012, 2013), in the tetraploid *Nicotiana tabacum.* Further work is needed to delineate the origin of the alkaloid biosynthetic pathway and that of the nicotinate and nicotinamide metabolism (Fig. 11) as contributors to nicotine biosynthesis and accumulation among the distinct *N. tomentosiformis* and *N. sylvestris* diploid tobacco species.

In the present work, the target genes investigated pertain to polyamine and alkaloid biosynthesis and the objective of this work was to test for the effect of their downregulation on leaf alkaloids and nicotine content. Expression of the genes examined is known to occur in all plant tissues and has been investigated in *Arabidopsis thaliana* (Jumtee et al. 2008; El Amrani et al. 2019). This was further confirmed by us via gene leaf expression analysis, using the appropriate software found in the ePlant tool (https://bar.utoronto.ca/eplant), developed by Waese et al. (2017). The latter is designed to explore and corroborate

gene expression and localization in different plant tissues. Additionally, localization of expression of these genes has been independently reported in the leaves of tobacco and tomato plants (Kwak and Lee 2001; Bortolotti et al. 2004).

Of interest in this work is also the observation of an earlier-than-wild type initiation of a senescence-like phenomenon in the primary fully expanded and mature leaves, observed mainly with AIC and secondarily with AO transformants (Fig. 10). On the basis of the pathway schematic of alkaloid biosynthesis in *Nicotiana tabacum* (Fig. 11), the AIC functions as an intermediate in the arginine and proline metabolism, whereas AO functions in the nicotinate and nicotinamide metabolism. A cross-talk between the two pathways is not evident on the basis of Fig. 11 and related biosynthetic pathway schematics in the literature, and the RNAi down-regulation of the corresponding *AIC* and *AO* genes does not bring about the same effect on intermediate metabolites. More research is needed to address the physiology and etiology of this senescence-like phenomenon in the primary fully-expanded and mature leaves of these transformants.

Results in this work serve as a guide for the selection of target genes and transformant lines with a consistently downregulated nicotine content. The RNAi method applied in this work provided a proof-of-concept, showing down-regulation in gene expression at the mRNA level and down-regulation in the corresponding amount of product accumulated. Important in the context of this study is the effect of RNAi application on nicotine levels, measured two weeks after the topping of fully-grown plants (Fig. 9). Topping and subsequent harvesting of mature leaves is a common agronomic practice that significantly impacts the transcript levels, yield, and quality of the product in various crop plants (Singh et al. 2015; Henry et al. 2019).

Author contribution statement RSP, CK, YS, DX, UW, and JAS envisioned this project. RSP and CK designed the RNAi vectors. DHM executed and AM supervised the research. DHM and AM wrote the manuscript. All authors read the manuscript.

Acknowledgements We thank Christina Wistrom and her staff for the greenhouse support she provided during the cultivation and growth of both the T0 and T1 tobacco plants. We also wish to thank Jason W. Flora, Mingda Zhang, and Jesse Frederick for reading and commenting on the manuscript. Funding was provided by UCB grant (85992-13618-44-ME1AM).

Compliance with ethical standards

Conflict of interest The authors declare that they have no conflict of interest.

Human participants and/or animals Research did not involve human and/or animal subjects. Experimental protocols in this work were approved by the UC Berkeley Committee on Laboratory and Environmental Biosafety (CLEB).

Informed consent All authors have read and approved the submission of this work.

References

Bai Y, Pattanaik S, Patra B, Werkman JR, Xie CH, Yuan L (2011) Flavonoid-related basic helix-loop-helix regulators, NtAn1a and NtAn1b, of tobacco have originated from two ancestors and are functionally active. Planta 234(2):363–375

Baldwin IT (1989) Mechanism of damage-induced alkaloid production in wild tobacco. J Chem Ecol 15:1661–1680

Bortolotti C, Cordeiro A, Alcázar R et al (2004) Localization of arginine decarboxylase in tobacco plants. Physiol Plant 120:84–92. https://doi.org/10.1111/j.0031-9317.2004.0216.x

Chintapakorn Y, Hamill JD (2007) Antisense-mediated reduction in ADC activity causes minor alterations in the alkaloid profile of cultured hairy roots and regenerated transgenic plants of *Nicotiana tabacum*. Phytochemistry 68:2465–2479

DeBoer KD, Dalton HL, Edward FJ, Hamill JD (2011) RNAi-mediated downregulation of ornithine decarboxylase (ODC) leads to reduced nicotine and increased anatabine levels in transgenic *Nicotiana tabacum* L. Phytochemistry 72:344–355

DeBoer KD, Dalton HL, Edward FJ, Ryan SM, Hamill JD (2013) RNAi-mediated down-regulation of ornithine decarboxylase (ODC) impedes wound-stress stimulation of anabasine synthesis in *Nicotiana glauca*. Phytochemistry 86:21–28

Dewey RE, Xie J (2013) Molecular genetics of alkaloid biosynthesis in *Nicotiana tabacum*. Phytochemistry 94:10–27

El Amrani A, Couée I, Berthomé R et al (2019) Involvement of polyamines in sucrose-induced tolerance to atrazine-mediated chemical stress in *Arabidopsis thaliana*. J Plant Physiol 238:1–11. https://doi.org/10.1016/j.jplph.2019.04.012

Goodspeed TH, Clausen RE (1928) Interspeeific hybridization in *Nicotiana*, VIII. The sylvestris-tomentosa-tabacum hybrid and its bearing on the origin of tobacco. Univ Calif Pub Bot 11(13):243–256

Gray JC, Kung SD, Wildman SG, Sheen SJ (1974) Origin of *Nicotiana tabacum* L. detected by polypeptide composition of fraction I protein. Nature 252:226–227

Henry JB, Vann MC, Lewis RS (2019) Agronomic practices affecting nicotine concentration in flue-cured tobacco: a review. Agron J 111:1–9

Jumtee K, Bamba T, Okazawa A et al (2008) Integrated metabolite and gene expression profiling revealing phytochrome A regulation of polyamine biosynthesis of *Arabidopsis thaliana*. J Exp Bot 59:1187–1200. https://doi.org/10.1093/jxb/ern026

Kajikawa M, Sierro N, Kawaguchi H, Bakaher N, Ivanov NV, Hashimoto T, Shoji T (2017) Genomic insights into the evolution of the nicotine biosynthesis pathway in tobacco. Plant Physiol 174(2):999–1011

Kirst H, Shen YX, Vamvaka E, Betterle N, Xu DM, Warek U, Strickland JA, Melis A (2018) Downregulation of the *CpSRP43* gene expression confers a truncated light-harvesting antenna (TLA) and enhances biomass and leaf-to-stem ratio in *Nicotiana tabacum* canopies. Planta 248:139–154

Kung SD, Sakano K, Gray JC, Wildman SG (1975) The evolution of fraction I protein during the origin of a new species of *Nicotiana*. J Mol Evol 7(1):59–64

Kwak SH, Lee SH (2001) The regulation of ornithine decarboxylase gene expression by sucrose and small upstream open reading frame in tomato (*Lycopersicon esculentum* Mill). Plant Cell Physiol 42:314–323. https://doi.org/10.1093/pcp/pce040

Leete E (1977) Biosynthesis and metabolism of the tobacco alkaloids. Proc Am Chem Soc Symp 173:365–388

Moghbel N, Ryu B, Ratsch A, Steadman KJ (2017) Nicotine alkaloid levels, and nicotine to nornicotine conversion, in Australian *Nicotiana* species used as chewing tobacco. Heliyon 3(11):e00469

Murashige T, Skoog F (1962) A revised medium for rapid growth and bioassays with tobacco tissue cultures. Physiol Plant 15:473–497

Patel RK, Patel JB, Trivedi PD (2015) Spectrophotometric method for the estimation of total alkaloids in the *Tinospora cordifolia* M. and its herbal formulations. Int J Pharm Pharm Sci 7:249–251

Patra B, Schluttenhofer C, Wu Y, Pattanaik S, Yuan L (2013) Transcriptional regulation of secondary metabolite biosynthesis in plants. Biochim Biophys Acta 11:1236–1247

Payyavula RS, Navarre DA, Kuhl J, Pantoja A (2013) Developmental effects on phenolic, flavonol, anthocyanin, and carotenoid metabolites and gene expression in potatoes. J Agric Food Chem 61(30):7357–7365

Payyavula RS, Navarre DA, Kuhl JC, Pantoja A, Pillai SS (2012) Differential effects of environment on potato phenylpropanoid and carotenoid expression. BMC Plant Biol 12:39. https://doi.org/10.1186/1471-2229-12-39

Saitoh F, Nona M, Kawashima N (1985) The alkaloid contents of sixty *Nicotiana* species. Phytochemistry 24:477–480

Singh SK, Wu Y, Ghosh JS, Pattanaik S, Fisher C, Wang Y, Lawson D, Yuan L (2015) RNA-sequencing reveals global transcriptomic changes in *Nicotiana tabacum* responding to topping and treatment of axillary-shoot control chemicals. Sci Rep 5:18148

Sisson VA, Severson RF (1990) Alkaloid composition of the *Nicotiana* species. Beitr Tabakforsch 14:327–339

Smith HH (1968) Recent cytogenetic studies in the genus *Nicotiana*. Adv Genet 14:1–54

Tayoub G, Sulaiman H, Alorfi M (2015) Determination of nicotine levels in the leaves of some *Nicotiana tabacum* varieties cultivated in Syria. Herba Pol 61(4):23–30

Tso TC, Jeffrey RN (1961) Biochemical studies on tobacco alkaloids. IV. The dynamic state of nicotine supplied to *N. rustica*. Arch Biochem Biophys 92:253–256

Waese J, Fan J, Pasha A et al (2017) ePlant: visualizing and exploring multiple levels of data for hypothesis generation in plant biology. Plant Cell 29:1806–1821. https://doi.org/10.1105/tpc.17.00073

Waller GR, Nowacki EK (1978) Alkaloid biology and metabolism in plants. Plenum Press, New York